Measurement of the differential cross section of Z boson production in association with jets at CMS

Qun WANG

School of Physics, Peking University (PKU)

On behalf of CMS Collaboration

CLHCP, 20 December 2018

Outline

1. Introduction
   - Motivation
   - Observables
2. Analysis
   - Data and simulation
   - Event selections
   - Theoretical Predictions for Cross Section
   - Results
3. Summary
4. Backup
   - TTbar Background Estimation
   - Detector Level Results
   - From Reco Distribution to Cross Section
   - Systematic Uncertainties

Motivation

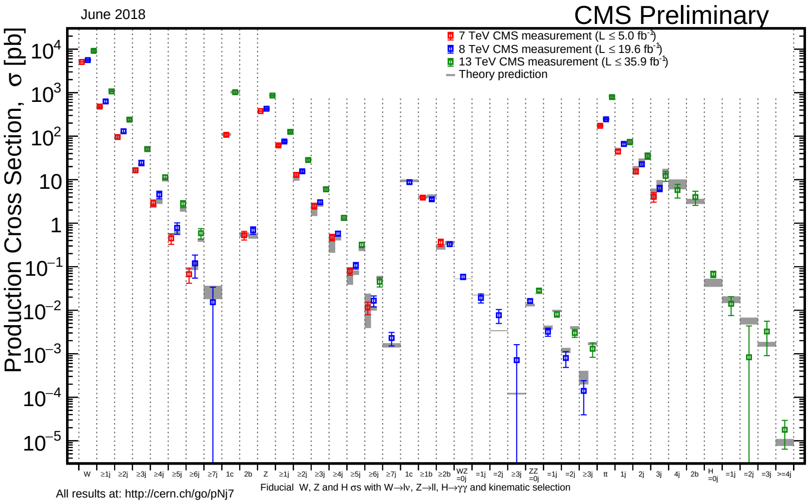

June 2018
CMS Preliminary
7 TeV CMS measurement (L ≤ 5.0 fb^{-1})
8 TeV CMS measurement (L ≤ 19.6 fb^{-1})
13 TeV CMS measurement (L ≤ 35.9 fb^{-1})
Theory prediction
Production Cross Section, σ [pb]
Fiducial W, Z and H σs with W→lν, Z→ll, H→γγ and kinematic selection
All results at: http://cern.ch/go/pNj7

Motivation

- Z+jets process provides fundamental tests of quantum chromodynamics (QCD)
- Precision measurement is crucial for deep understanding and modelling of QCD interactions.
  - important for modeling the production mechanism involved in the Higgs boson and new physics searches (e.g. Supersymmetry).
- This process is a standard candle at LHC:
  - High cross section.
  - Almost background-free.
  - Clean signature.
- It is a dominant background in many SM processes, such as Higgs production, $t\bar{t}$ production and for searches beyond SM.
- Comparison with predictions motivates Monte Carlo generator development and improves our understanding of the prediction uncertainties.

Observables

First time at 13 TeV:

- Exclusive and inclusive jet multiplicities for N_jets $\geq$ 0, 1, 2, 3
- Z boson p_{T} for N_jets $\geq$ 0, 1
- Transverse momenta p_{T} of the jet for N_jets $\geq$ 1, 2, 3
- Rapidity (η) of the jet for N_jets $\geq$ 1, 2, 3
- Scalar sum of the jets transverse momentum (H_T) for N_jets $\geq$ 1, 2, 3
- p_{T} balance between the Z boson and the reconstructed jets: $p_{\mathrm{T}}^{bal} = |\overrightarrow{p_{\mathrm{T}}}(Z) + \sum_{jets} \overrightarrow{p_{\mathrm{T}}}(j_i)|$
- Jets-Z balance (JZB): JZB$=|\sum_{jets} \overrightarrow{p_{\mathrm{T}}}(j_i)| - |\overrightarrow{p_{\mathrm{T}}}(Z)|$

This analysis is published in Eur. Phys. J. C78 (2018) 965, arXiv:1804.05252.

Data and simulation

Data: collected in 2015 at $\sqrt{s} = 13$ TeV in proton-proton collisions, with integrated luminosity: 2.19 fb^{-1}.

MC signal: NLO MG5_aMC@NLO

- Signal is generated by MG5_aMC@NLO using FxFx merging scheme with dilepton mass larger than 50 GeV.
- The matrix elements include Z+0/1/2 partons NLO computation; Z+3 parton LO approximation.
- The parton shower and hadronization are held by PYTHIA8 using CUETP8M1.
- PDF sets: NNPDF 3.0 is used and the coupling constant $\alpha_s(m_Z)$ is set to 0.118.

MC background: $t\bar{t}$, single top, double vector boson (VV) and Wjets samples.

Event selections

Unprescaled dimuon/di-electron triggers:

- HLT_Mu17_TrkIsoVVL_Mu8(TkMu8)_TrkIsoVVL_DZ
- HLT_Ele17_Ele12_CaloIdL_TrackIdL_IsoVL_DZ

Event selections:

- mu: $p_{\mathrm{T}}(l) \geq 20$ GeV, $|\eta| < 2.4$, tight muon identification, PFIsoCorr ≤ 0.25.
- ele: $p_{\mathrm{T}}(l) \geq 20$ GeV, $|\eta| \leq 1.442$, $1.566 \leq |\eta| \leq 2.4$, medium identification, PFIsoCorr ≤ 0.15.
- on-shell Z boson: $71 \leq m_{l^+l^-} \leq 111$ GeV.
- Anti-k$_T$(R=0.4) jets: $p_{\mathrm{T}} \geq 30$ GeV, $|\eta| < 2.4$, $\Delta R(j,l) > 0.4$, puMVA$\geq$ -0.2

backgroud estimation:

- $t\bar{t}$, data-driven method.
- other backgrounds (single Top, VV, W+jets), from MC.

Measurements are unfolded to generator level.

Theoretical Predictions for Cross Section

MADGRAPH5_aMC@NLO + PYTHIA8 (NLO MG5_aMC)

- NLO matrix element up to 2 partons, FxFx jet matching
- NNPDF3.0 NLO PDF, CUETP8M1 Pythia8 tune

MADGRAPH5_aMC@NLO + PYTHIA8 (LO MG5_aMC)

- LO matrix element up to 4 partons, k_T-MLM merging
- NNPDF PDF, CUETP8M1 Pythia8 tune

Z+1 jet fixed order NNLO (N_{jetti} NNLO)

- Correction for hadronization, parton shower and multiple parton interaction computed with MADGRAPH5_aMC@NLO + PYTHIA8
- CT14 PDF

GENEVA

- NNLL'+NNLO matched to PS
- PDF4LHC15 NNLO, specific PYTHIA8 tune based on CUETP8M1

Table: Predictions at different accuracies. While the matrix elements are calculated at LO, NLO or NNLO, other additional jets described using PYTHIA8 (*PY*).

Prediction	no jet	1 jet	2 jets	3 jets	4 jets
MG5_aMC (LO)	LO	LO	LO	LO	LO
MG5_aMC (NLO)	NLO	NLO	NLO	LO	*PY*
GENEVA	NNLO	NLO	LO	*PY*	*PY*
Z+1 jet at NNLO	-	NNLO	NLO	LO	

Results-jet multiplicity, Z p_T

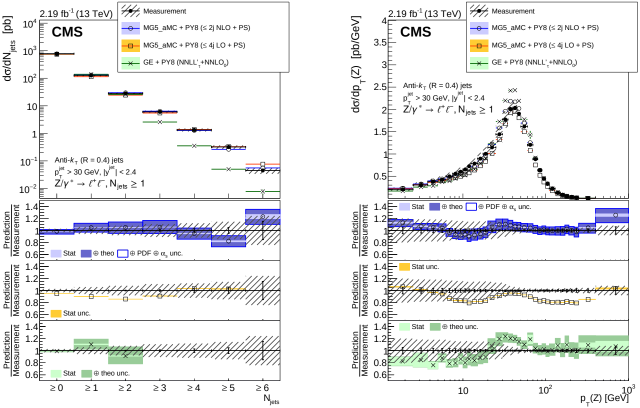

- The NLO MG5_AMC prediction shows agreement with the measurement.
- The LO MG5_AMC prediction tends to be lower than NLO MG5_AMC.
- While GENEVA describes the measured cross section up to $N_{jets} = 2$.
- GENEVA describes the shape of the distribution in the region below 10GeV for $N_{jets} \geq 1$.

Results-jet transverse momentum

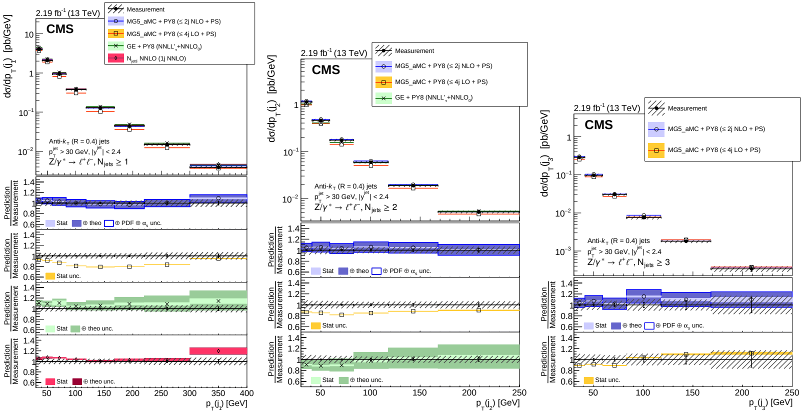

- The LO MG5_aMC prediciton differs from the measurement, showing a steeper slope in the low p_T region.
- This discrepancy disappears for NLO MG5_aMC, N_{jetti} NNLO when adding NLO terms.
- GENEVA prediction is in good agreement for the p_T of the first leading jet.

Results-p_T balance, JZB

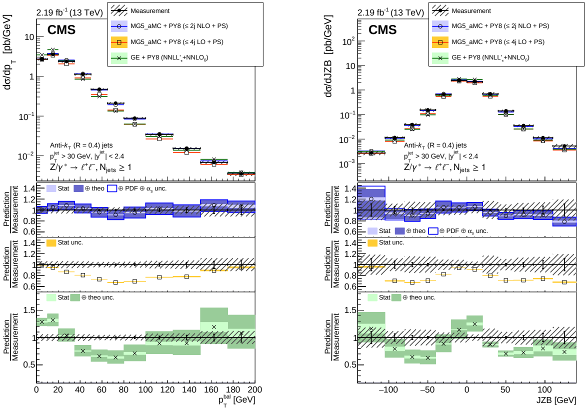

- The measurement is in good agreement with the NLO MG5_aMC.
- The LO MG5_aMC does not fully describe the data for the process with at least two jets.
- GENEVA does not manage to describe the p_T^{bal} or JZB variable.
- This indicates the importance of the NLO correction.

Summary

- The differential cross section of Z+jets has been measured as a function of Z p_{T}, jet multiplicities, jet transverse momentum, jet rapidity, jet H_T, p_{T} balance and JZB.
- Four type of theoretical predictions have been compared to measurement: LO MG5_aMC, NLO MG5_aMC, N$_{jetti}$ NNLO and GENEVA.
- The NLO multiparton calculation by MG5_aMC@NLO interfaced with PYTHIA8 gives better descriptions.
- GENEVA shows good agreement with measurement with accurancy at NLO ($N_{jets} \geq 1$), while for LO accurancy it still needs to be improved.
- The measurement results suggest to use multiparton NLO predictions to estimate the Z + jets at CMS in the SM measurement and searches, along with its associated uncertainties.

Backup

Thanks!

TTbar Background Estimation

- $e - \mu$ channel is used to estimated $t\bar{t}$ background, replaced double muon trigger with single muon trigger HLT_IsoTkMu20.
- The $t\bar{t}$ MC simulation is reweighted by a "TTbar scale factor" defined as:

$$\mathcal{C} = \frac{Data - X}{MC_{t\bar{t}}}$$

X: MC signal and the other MC backgrounds except $t\bar{t}$.

N_{jets}	$\mathcal{C}$	uncertainty
1	0.94	$\pm$ 0.04
2	0.97	$\pm$ 0.03
3	1.01	$\pm$ 0.04
4	0.86	$\pm$ 0.06
5	0.61	$\pm$ 0.09
6	0.68	$\pm$ 0.17

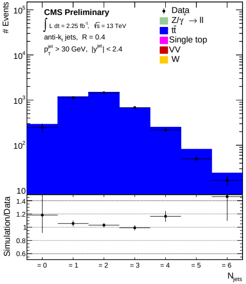

Detector Level Results

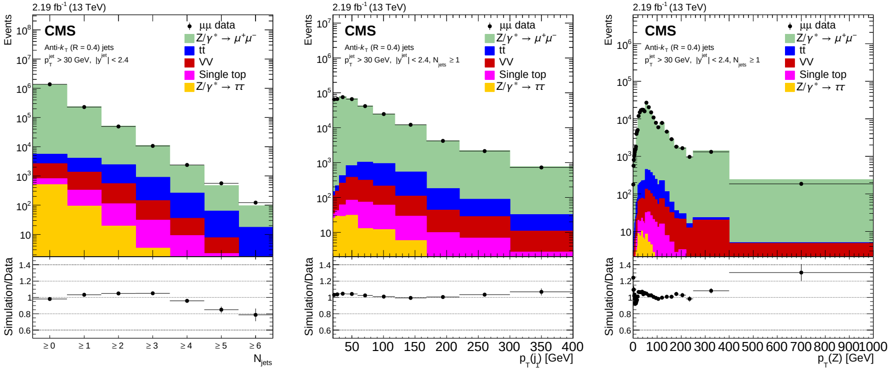

Data to simulation comparison of the inclusive jet multiplicity (left), the p_T of first leading jet (middle), and Z p_T with $N_{jets} \geq 1$ (right).

Detector Level Results

The defination of p_T balance and JZB: $p_T^{bal} = |\vec{p_T}(Z) + \sum_{jets} \vec{p_T}(j_i)|$
JZB$=|\sum_{jets} \vec{p_T}(j_i)| - |\vec{p_T}(Z)|$

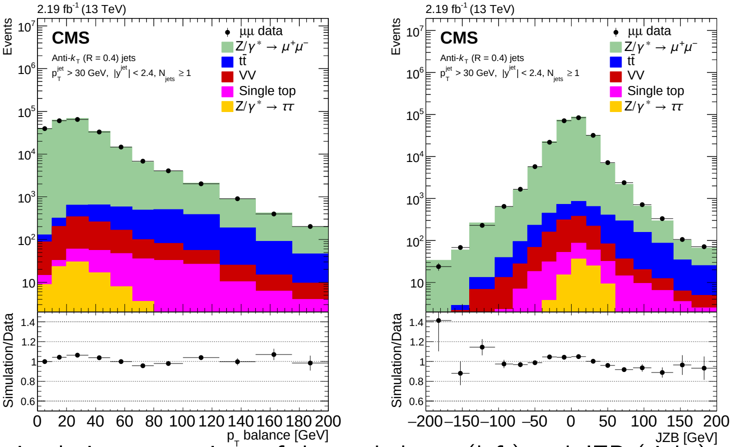

Data to simulation comparison of the p_T balance (left) and JZB (right) with N_jets $\geq$1.

From Reco Distribution to Cross Section

- Background subtraction
  Data signal = data - background (from MC)
- Fake subtraction
  Data signal - fakes = Data signal - Fakes (from MC)
- Detector effect correction
  - Data points differs from their true values due to detector effects.
  - Unfolding [1] is used to estimate *Gen* distributions from *Reco*.
  - Response Matrices are obtained from the NLO MG5_aMC.
- Phase space at generator level:
  - $p_T(l) \geq 20$ GeV, $|\eta(l)| < 2.4$
  - $p_T(j) \geq 30$ GeV, $|\eta(j)| < 2.4$, $\Delta R(j, l) > 0.4$

[1] Iterative D'Agostini method

Systematic Uncertainties

- Jet energy scale (JES): 4% for $N_{jets} \geq 1$
- Jet energy resolution (JER): below 1%
- Efficiency Correction (Eff): 2% to 4% for the large $p_{\mathrm{T}}(lepton)$
- Luminosity (Lumi): 2.3%
- Background estimation (Bkg): less than 1% for $N_{jets} \leq 4$
- Lepton energy scale (LES) and resolution (LER): quite small, 0.3%.
- Pileup (PU): Varying the min. bias cross section 71mb by $\pm$5%, results in 1%
- Unfolding (Unf): *Unfmodel*, the difference between the nominal results and the unfolded results; *Unfstat*, an additional uncertainty comes from the finite size of the simulation sample used to build the response matrix

All these systematic uncertainties are added in quadrature assuming each uncertainty source is independent, yielding to the total systematic uncertainty.

- PU MVA cut is applied to minimize the dependence on number of vertices.
- We are using the loose working point with puMVA $>$ -0.2

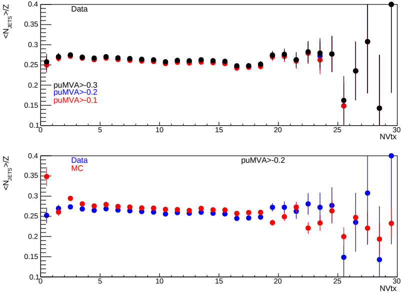

Trigger Scale Factor

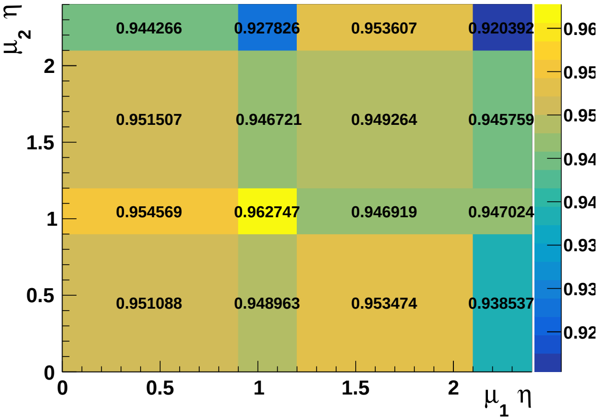

Detector Level Results

Pileup distribution after reweighting on MC samples using a minimum bias p-p cross-section of 69 mb.

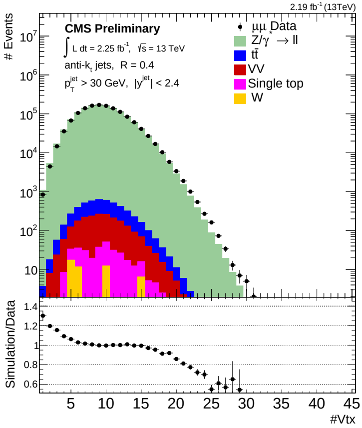

Detector Level Results

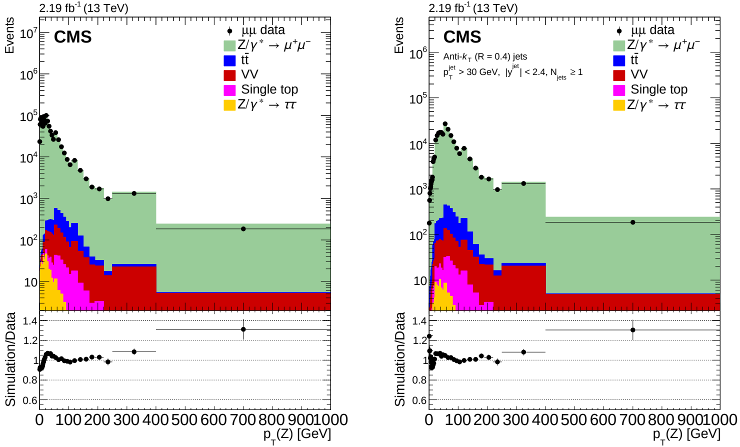

Data to simulation comparison of Z p_T with $N_{jets} \geq 0$ (left) and 1 (right).

Detector Level Results

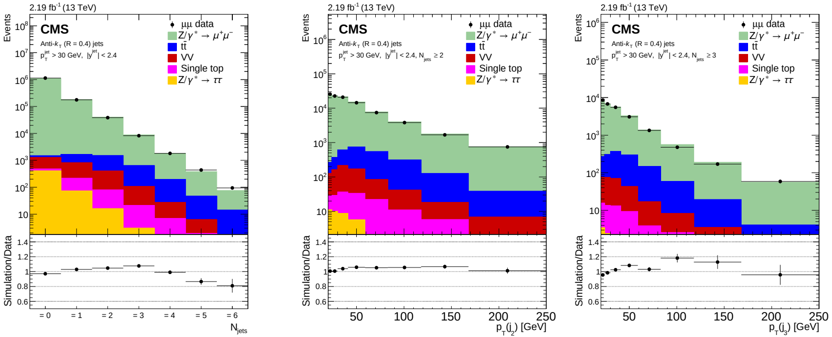

Data to simulation comparison of the exclusive jet multiplicity (left), and the p_T of second leading jet (middle) and third leading jet (right).

Detector Level Results

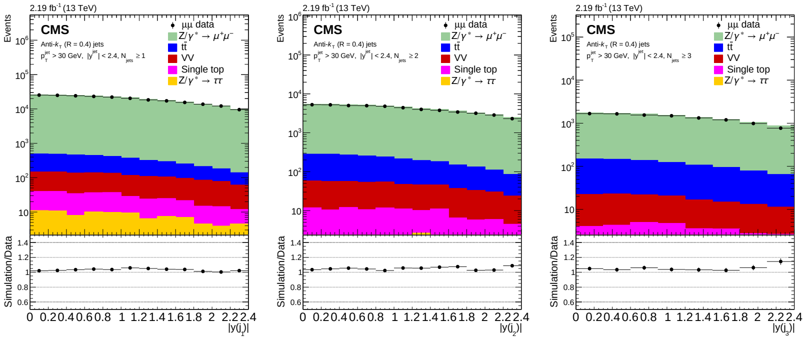

Data to simulation comparison of jet rapidity distributions for the 3 first jets.

Detector Level Results

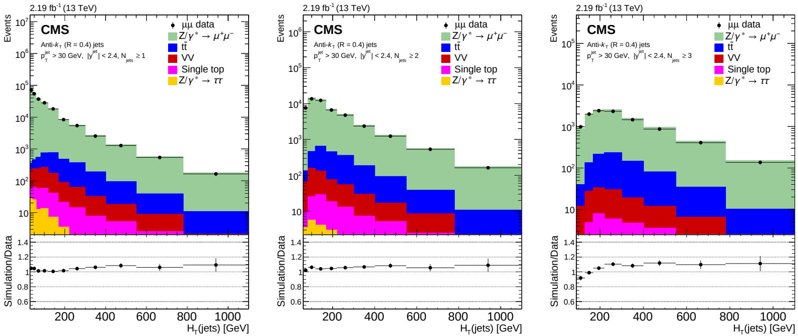

Data to simulation comparison of H_T of the jets for inclusive jet multiplicities of 1 (left), 2 (middle) and 3 (right) obtained for the $\mu\mu$ sample.

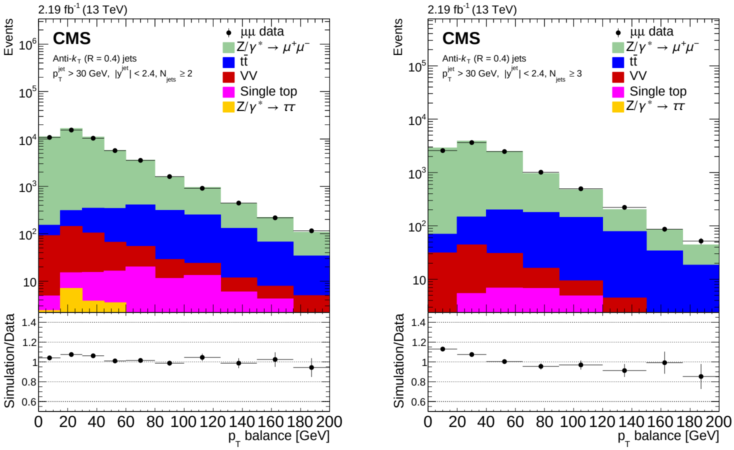

Data to simulation comparison of the p_T balance for N_jets $\geq$ 2 and 3, respectively.

Detector Level Results

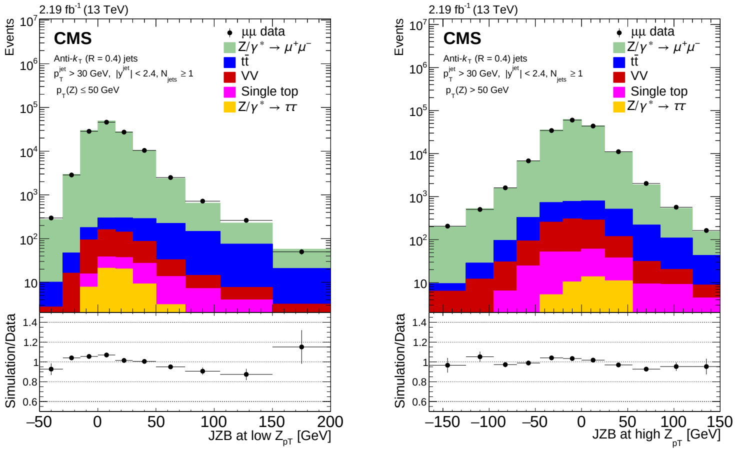

Data to simulation comparison of the JZB for N_jets ≥ 2 and 3, respectively.

Response Matrix

Percentage of Reco events in bin *i* from Gen events in *j* (row normalisation).
One chooses binning optimized considering statistics and resolution (purity above 60%).
The steps of bins is important to avoid the large uncertainty from unfolding.

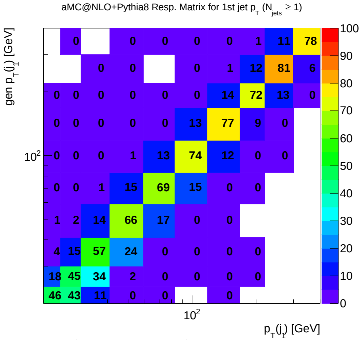

Figure: Response matrix used for the unfolding procedure for the variable of the jet exclusive multiplicity for the $\mu\mu$ channel. Numbers are expressed in percents.

Matrix elements

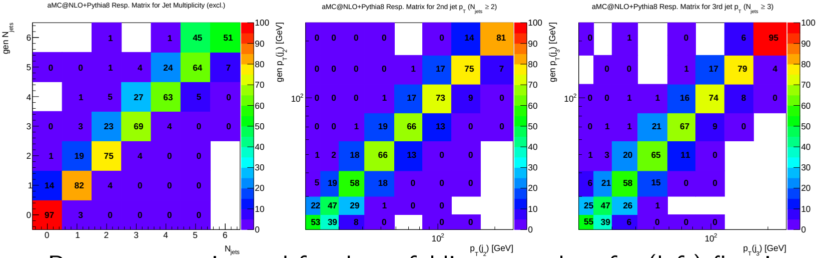

Figure: Response matrix used for the unfolding procedure for (left) first jet transverse momentum, (middle) second jet transverse momentum and (right)the third jet transverse momentum for $\mu\mu$ channel. Numbers are expressed in percents.

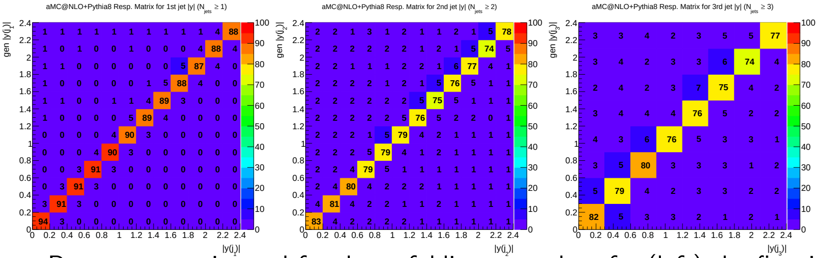

Figure: Response matrix used for the unfolding procedure for (left) the first jet rapidity, (middle) second jet rapidity and (right) third jet rapidity for $\mu\mu$ channel.

Channel Comparison

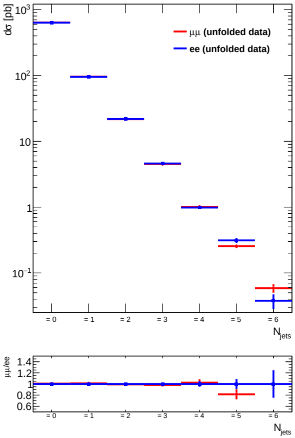

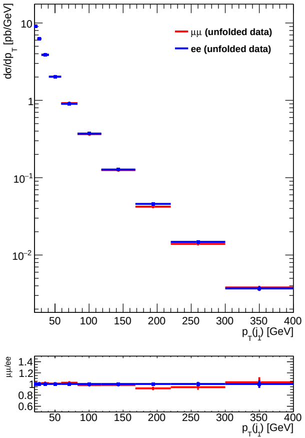

Comparison with CMS inclusive cross section measurement:

- Using the fiducial region as SMP-15-004, with 43 ± 2 pb^{-1}, with 50 ns

Channel Comparison

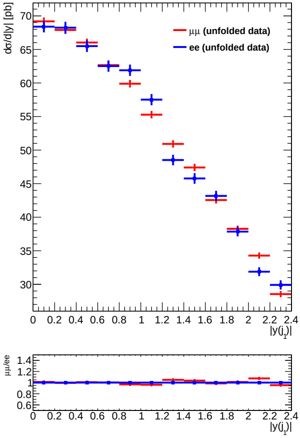

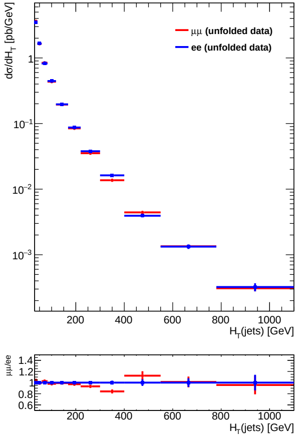

Results-jet multiplicity

Table: Differential cross section in exclusive jet multiplicity for the combination of both decay channels and break down of the systematic uncertainties.

N_{jets}	$\frac{d\sigma}{dN_{jets}}$ [pb]	Tot. unc [%]	Stat [%]	JES [%]	JER [%]	Eff [%]	Lumi [%]	Bkg [%]	pileup [%]	Unf model [%]	Unf stat [%]
$= 0$	652	3.0	0.091	1.1	0.046	1.5	2.3	< 0.01	0.22	-	0.026
$= 1$	97.9	5.1	0.27	4.3	0.18	1.5	2.3	0.012	0.30	-	0.10
$= 2$	22.2	7.3	0.63	6.7	0.20	1.6	2.3	0.026	0.43	-	0.26
$= 3$	4.68	10	1.4	9.9	0.39	1.7	2.3	0.13	0.29	-	0.54
$= 4$	1.01	11	3.5	10	0.24	1.7	2.3	0.43	0.56	-	1.4
$= 5$	0.275	14	5.0	12	0.081	2.0	2.3	1.2	0.29	-	2.2
$= 6$	0.045	24	15	17	0.36	1.8	2.4	3.5	1.7	-	6.6

Table: Predictions at different accuracies. While the matrix elements are calculated at LO, NLO or NNLO, other additional jets described using PYTHIA8 (*PY*).

Prediction	no jet	1 jet	2 jets	3 jets	4 jets
MG5_AMC (LO)	LO	LO	LO	LO	LO
MG5_AMC (NLO)	NLO	NLO	NLO	LO	*PY*
GENEVA	NNLO	NLO	LO	*PY*	*PY*
Z+1 jet at NNLO	-	NNLO	NLO	LO	-

Results-jet multiplicity

Table: Differential cross section in inclusive jet multiplicity for the combination of both decay channels and break down of the systematic uncertainties.

N_{jets}	$\frac{d\sigma}{dN_{jets}}$ [pb]	Tot. unc [%]	Stat [%]	JES [%]	JER [%]	Eff [%]	Lumi [%]	Bkg [%]	pileup [%]	Unf model [%]	Unf stat [%]
≥ 0	778	2.8	0.081	0.079	< 0.01	1.5	2.3	< 0.01	0.24	-	0.025
≥ 1	126.2	5.7	0.23	5.0	0.19	1.5	2.3	< 0.01	0.32	-	0.085
≥ 2	28.3	8.0	0.52	7.4	0.22	1.6	2.3	0.073	0.41	-	0.21
≥ 3	6.01	11	1.1	10	0.29	1.7	2.3	0.25	0.35	-	0.46
≥ 4	1.33	12	2.8	11	0.16	1.7	2.3	0.66	0.54	-	1.1
≥ 5	0.320	14	4.8	13	0.10	1.9	2.3	1.5	0.48	-	2.1
≥ 6	0.045	24	15	17	0.36	1.8	2.4	3.5	1.7	-	6.6

Results-Z p_T

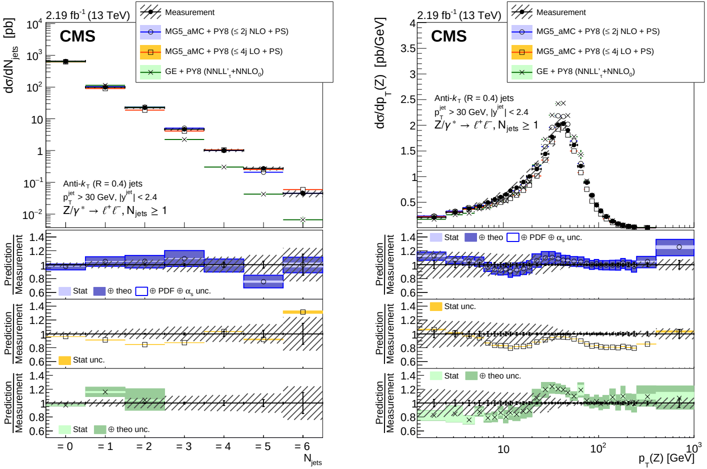

- NLO MG5_aMC is best in describing the data.
- LO MG5_aMC tends to be lower than NLO MG5_aMC.
- GENEVA describes the shape of the distribution in the region below 10 GeV for $N_{jets} \geq 1$.

Table: Differential cross section in 1st jet p_T ($N_{jets} \geq 1$) and break down of the systematic uncertainties for the combination of both decay channels.

$p_T(j_1)$ [GeV]	$\frac{d\sigma}{dp_T(j_1)}$ [$\frac{pb}{GeV}$]	Tot. Unc [%]	Stat [%]	JES [%]	JER [%]	Eff [%]	Lumi [%]	Bkg [%]	PU [%]	Unf model [%]	Unf stat [%]
30 – 41	3.99	5.8	0.30	5.0	0.17	1.5	2.3	0.0081	0.38	0.34	0.11
41 – 59	2.07	5.3	0.36	4.4	0.18	1.5	2.3	0.012	0.33	0.35	0.13
59 – 83	0.933	5.1	0.45	4.2	0.17	1.6	2.3	0.015	0.25	0.26	0.18
83 – 118	0.377	5.1	0.60	4.1	0.20	1.6	2.3	0.051	0.28	0.24	0.24
118 – 168	0.1301	5.1	0.93	4.1	0.22	1.6	2.3	0.070	0.057	0.31	0.38
168 – 220	0.0448	4.9	1.4	3.7	0.21	1.6	2.3	0.077	0.21	0.30	0.59
220 – 300	0.01477	6.4	2.0	5.3	0.32	1.6	2.3	0.066	0.30	0.37	0.85
300 – 400	0.00390	7.0	3.4	5.2	0.24	1.7	2.3	0.097	0.28	0.72	1.4

Results-jet transverse momentum

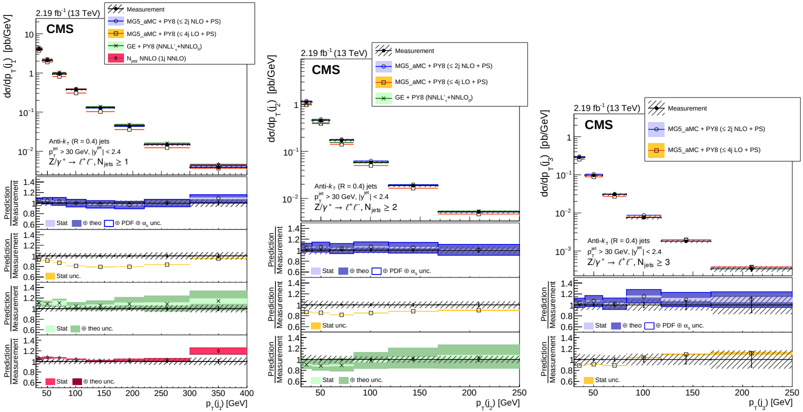

- The LO MG5_aMC prediciton differs from the measurement, showing a steeper slope in the low p_T region.
- This discrepancy disappears for NLO MG5_aMC, N_{jetti} NNLO when adding NLO terms.
- GENEVA prediction is in good agreement for the p_T of the first leading jet.

Results-jet rapidity

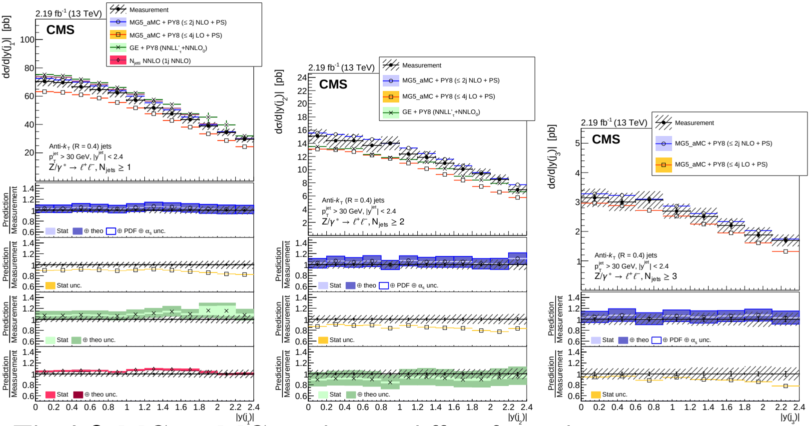

- The LO MG5_aMC prediciton differs from the measurement, showing a steeper slope in the low p_T region.
- This discrepancy disappears for NLO MG5_aMC, N$_{jetti}$ NNLO when adding NLO terms.
- GENEVA prediction is in good agreement for the p_T of the first

Table: Differential cross section in 1st jet $|\eta|$ ($N_{\text{jets}} \geq 1$) and break down of the systematic uncertainties for the combination of both decay channels.

$\lvert y(j_1)\rvert$	$\frac{d\sigma}{d\lvert y(j_1)\rvert}$ [pb]	Tot. Unc [%]	Stat [%]	JES [%]	JER [%]	Eff [%]	Lumi [%]	Bkg [%]	PU [%]	Unf model [%]	Unf stat [%]
0 – 0.2	70.4	4.9	0.70	3.9	0.075	1.5	2.3	0.016	0.23	0.11	0.25
0.2 – 0.4	69.6	4.9	0.72	4.0	0.084	1.5	2.3	0.016	0.28	0.14	0.26
0.4 – 0.6	66.7	5.0	0.73	4.1	0.12	1.5	2.3	0.015	0.18	0.14	0.26
0.6 – 0.8	64.6	5.2	0.72	4.3	0.17	1.6	2.3	0.014	0.30	0.15	0.26
0.8 – 1	62.4	5.1	0.77	4.2	0.071	1.5	2.3	0.013	0.19	0.17	0.28
1 – 1.2	57.2	5.1	0.82	4.2	0.19	1.5	2.3	0.012	0.29	0.24	0.29
1.2 – 1.4	51.7	5.4	0.88	4.5	0.17	1.5	2.3	0.0088	0.28	0.25	0.31
1.4 – 1.6	47.6	6.2	0.91	5.5	0.073	1.5	2.3	0.0057	0.31	0.31	0.32
1.6 – 1.8	43.5	6.5	0.94	5.7	0.22	1.5	2.3	0.0037	0.35	0.21	0.34
1.8 – 2	39.0	6.9	0.98	6.2	0.40	1.5	2.3	0.0031	0.41	0.32	0.35
2 – 2.2	34.4	7.5	1.1	6.8	0.47	1.5	2.3	0.0034	0.68	0.40	0.39
2.2 – 2.4	29.6	7.6	1.2	6.8	0.74	1.5	2.3	0.0079	0.75	0.35	0.44

Results-jet H_T

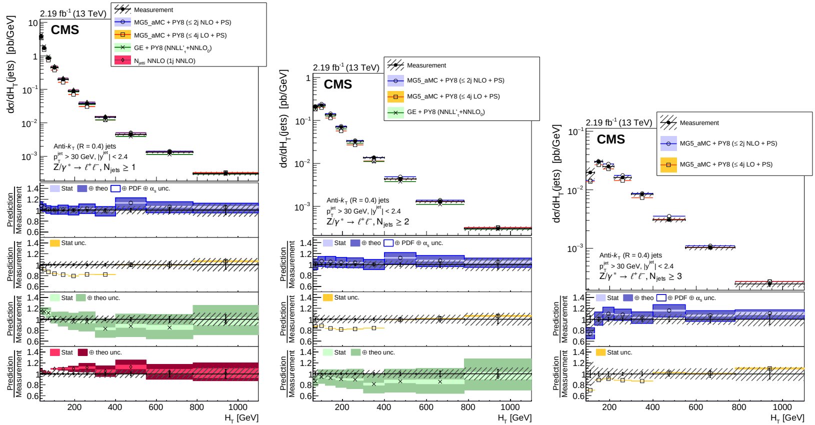

- The LO $\mathrm{MG5\_AMC}$ prediciton differs from the measurement, showing a steeper slope in the low p_T region.
- This discrepancy disappears for NLO $\mathrm{MG5\_AMC}$, N$_{jetti}$ NNLO when adding NLO terms.
- GENEVA prediction is in good agreement for the p_T of the first

Table: Differential cross section in H_T ($N_{jets} \geq 1$) and break down of the systematic uncertainties for the combination of both decay channels.

H_T [GeV]	$\frac{d\sigma}{dH_T}$ [$\frac{pb}{GeV}$]	Tot. Unc [%]	Stat [%]	JES [%]	JER [%]	Eff [%]	Lumi [%]	Bkg [%]	PU [%]	Unf model [%]	Unf stat [%]
30 – 41	3.66	6.2	0.68	5.4	0.21	1.5	2.3	0.018	0.40	0.92	0.20
41 – 59	1.684	4.6	0.60	3.5	0.15	1.5	2.3	0.0048	0.26	1.1	0.22
59 – 83	0.852	5.3	0.73	4.4	0.23	1.5	2.3	0.0054	0.29	0.64	0.28
83 – 118	0.449	6.1	0.78	5.3	0.12	1.6	2.3	0.015	0.35	0.55	0.31
118 – 168	0.198	5.9	0.98	5.1	0.20	1.6	2.3	0.040	0.17	0.40	0.40
168 – 220	0.0887	6.3	1.6	5.3	0.37	1.6	2.3	0.078	0.36	0.32	0.64
220 – 300	0.0373	6.9	1.7	6.0	0.095	1.7	2.3	0.14	0.20	0.17	0.68
300 – 400	0.0149	6.8	2.4	5.6	0.21	1.6	2.3	0.20	0.17	0.21	1.0
400 – 550	0.00448	7.4	3.3	5.7	0.21	1.8	2.3	0.36	0.64	0.29	1.3
550 – 780	0.00134	8.2	5.4	4.8	0.15	1.6	2.3	0.40	1.2	0.23	2.1
780 – 1100	0.000306	12.	8.2	7.5	0.22	1.8	2.3	0.59	0.70	0.56	3.2

Table: Differential cross section in H_{T} ($N_{\mathrm{jets}} \geq 2$) and break down of the systematic uncertainties for the combination of both decay channels.

H_{T} [GeV]	$\frac{d\sigma}{dH_{\mathrm{T}}}$ [$\frac{\mathrm{pb}}{\mathrm{GeV}}$]	Tot. Unc [%]	Stat [%]	JES [%]	JER [%]	Eff [%]	Lumi [%]	Bkg [%]	PU [%]	Unf model [%]	Unf stat [%]
60 – 83	0.212	11.	2.2	10.	0.27	1.5	2.3	0.093	0.67	0.96	0.68
83 – 118	0.227	7.9	1.1	7.2	0.12	1.6	2.3	0.063	0.45	0.63	0.42
118 – 168	0.1370	6.7	1.1	5.9	0.18	1.6	2.3	0.038	0.31	0.59	0.42
168 – 220	0.0705	7.3	1.4	6.5	0.29	1.6	2.3	0.11	0.36	0.31	0.57
220 – 300	0.0329	7.1	1.6	6.2	0.11	1.7	2.3	0.16	0.18	0.29	0.64
300 – 400	0.01360	6.8	2.2	5.7	0.20	1.6	2.3	0.22	0.33	0.29	0.90
400 – 550	0.00436	7.3	3.1	5.8	0.18	1.8	2.3	0.37	0.57	0.28	1.2
550 – 780	0.00129	8.1	5.1	5.1	0.17	1.6	2.3	0.41	1.1	0.21	1.9
780 – 1100	0.000304	12.	8.0	7.2	0.25	1.7	2.3	0.58	0.67	0.41	3.1

Table: Differential cross section in H_T ($N_{jets} \geq 3$) and break down of the systematic uncertainties for the combination of both decay channels.

H_T [GeV]	$\frac{d\sigma}{dH_T}$ [$\frac{pb}{GeV}$]	Tot. Unc [%]	Stat [%]	JES [%]	JER [%]	Eff [%]	Lumi [%]	Bkg [%]	PU [%]	Unf model [%]	Unf stat [%]
90 – 130	0.0198	22.	6.6	20.	1.0	1.5	2.3	0.19	0.99	5.2	2.2
130 – 168	0.0301	12.	3.7	11.	0.35	1.7	2.3	0.15	0.39	2.1	1.2
168 – 220	0.0250	11.	3.6	9.5	0.17	1.7	2.3	0.19	0.42	0.74	1.2
220 – 300	0.0162	9.2	2.7	8.2	0.29	1.7	2.3	0.29	0.20	0.73	1.0
300 – 400	0.00842	8.4	3.3	7.0	0.12	1.7	2.3	0.37	0.24	0.43	1.3
400 – 550	0.00306	8.8	4.1	7.0	0.22	1.8	2.3	0.55	0.73	0.40	1.5
550 – 780	0.00103	10.	6.5	6.7	0.34	1.7	2.3	0.54	1.1	0.22	2.5
780 – 1100	0.000246	13.	9.3	6.4	0.17	1.7	2.3	0.68	0.91	2.7	3.5

$p_T(Z)$ [GeV]	$\frac{d\sigma}{dp_T(Z)}$ [$\frac{pb}{GeV}$]	Tot. unc [%]	Stat [%]	JES [%]	JER [%]	Eff [%]	Lumi [%]	Bkg [%]	LES [%]	LER [%]	pileup [%]	Unf model [%]	Unf stat [%]
0 — 1.25	0.066	27	9.4	24	1.6	1.6	2.3	<0.1	1.9	1.4	0.62	5.9	2.2
1.25 — 2.5	0.205	20	5.4	19	1.5	1.6	2.3	<0.1	1.1	0.57	0.56	2.0	1.3
2.5 — 3.75	0.305	18	4.3	18	1.2	1.5	2.3	<0.1	0.95	0.46	0.27	1.7	1.1
3.75 — 5	0.376	18	3.7	17	1.3	1.6	2.3	<0.1	1.2	0.27	0.69	1.2	1.0
5 — 6.25	0.422	18	3.6	17	1.2	1.5	2.3	<0.1	0.93	0.14	0.76	1.7	1.1
6.25 — 7.5	0.498	17	3.3	16	1.1	1.5	2.3	<0.1	0.85	0.14	0.55	1.7	1.0
7.5 — 8.75	0.556	16	3.0	15	1.0	1.5	2.3	<0.1	0.88	0.10	0.51	2.0	0.99
8.75 — 10	0.601	15	2.8	14	0.95	1.6	2.3	<0.1	0.94	0.060	0.33	2.7	0.93
10 — 11.25	0.65	16	2.7	15	0.86	1.6	2.3	<0.1	0.99	0.035	0.33	3.1	0.91
11.25 — 12.5	0.73	14	2.6	13	0.92	1.5	2.3	<0.1	0.83	0.15	0.31	3.3	0.91
12.5 — 15	0.78	15	2.0	14	1.1	1.6	2.3	<0.1	0.74	0.13	0.33	2.8	0.71
15 — 17.5	0.89	15	2.0	14	1.1	1.5	2.3	<0.1	1.5	0.14	0.094	2.3	0.69
17.5 — 20	1.00	15	1.9	15	1.1	1.5	2.3	<0.1	1.2	0.016	0.17	1.1	0.65
20 — 25	1.15	14	1.3	14	1.1	1.6	2.3	<0.1	1.1	0.062	0.14	1.3	0.42
25 — 30	1.44	13	1.2	13	0.74	1.6	2.3	<0.1	0.97	0.022	0.31	1.3	0.36
30 — 35	1.77	10	1.0	9.8	0.39	1.5	2.3	<0.1	0.71	0.036	0.47	1.9	0.32
35 — 40	2.01	7.6	0.84	6.7	0.13	1.6	2.3	<0.01	0.34	0.059	0.36	1.6	0.28
40 — 45	2.04	6.0	0.82	5.0	0.067	1.6	2.3	<0.01	0.14	0.049	0.38	1.5	0.28
45 — 50	1.905	4.9	0.81	3.7	0.030	1.6	2.3	<0.01	0.19	0.034	0.40	1.0	0.29
50 — 60	1.616	3.8	0.63	2.4	0.038	1.5	2.3	0.012	0.23	0.039	0.42	0.74	0.23
60 — 70	1.204	3.3	0.71	1.4	0.031	1.6	2.3	0.018	0.52	0.031	0.22	0.53	0.26
70 — 80	0.881	3.2	0.79	0.93	0.022	1.6	2.3	0.024	0.66	0.024	0.38	0.52	0.30
80 — 90	0.634	3.3	0.89	0.55	0.015	1.6	2.3	0.028	0.94	0.0024	0.25	0.62	0.35
90 — 100	0.444	3.3	1.1	0.30	0.025	1.6	2.3	0.031	0.81	0.0024	0.36	0.74	0.42
100 — 110	0.334	3.3	1.2	0.28	0.0080	1.6	2.3	0.026	0.67	0.0022	0.25	0.77	0.48
110 — 130	0.2213	3.3	1.0	0.17	0.0070	1.6	2.3	0.021	0.88	0.019	0.20	0.79	0.41
130 — 150	0.1308	3.4	1.3	0.11	0.010	1.7	2.3	0.022	0.88	0.023	0.076	0.88	0.54
150 — 170	0.0813	3.6	1.6	0.14	0.012	1.7	2.3	0.016	0.76	0.027	0.12	1.0	0.67
170 — 190	0.0516	3.9	2.0	0.091	0.017	1.8	2.3	0.022	0.87	0.017	0.17	1.1	0.84
190 — 220	0.0317	4.0	2.2	0.088	0.0084	1.8	2.3	0.035	0.69	0.033	0.10	1.1	0.90
220 — 250	0.01836	4.5	2.8	0.041	0.0031	1.8	2.3	0.041	0.83	0.020	0.11	1.4	1.2
250 — 400	0.00508	4.5	2.6	0.022	0.0037	2.0	2.3	0.065	0.80	0.0046	0.12	1.4	1.1
400 — 1000	0.000187	7.9	6.2	0.019	0.00077	1.7	2.4	0.11	1.7	0.065	0.58	2.6	2.4